Title

Phosphorylation of p53 by TAF1 Inactivates p53-Dependent Transcription in the DNA Damage Response

Journal

Molecular Cell, 53(1)

ISSN

1097-2765

Authors

Wu, Yong
Lin, Joy C
Piluso, Landon G
et al.

Publication Date

2014

DOI

10.1016/j.molcel.2013.10.031

Peer reviewed

Molecular Cell
Article

Phosphorylation of p53 by TAF1 Inactivates p53-Dependent Transcription in the DNA Damage Response

Yong Wu,[1] Joy C. Lin,[1] Landon G. Piluso,[1] Joseph M. Dhahbi,[1] Selene Bobadilla,[1] Stephen R. Spindler,[1] and Xuan Liu[1,*]
[1]Department of Biochemistry, University of California, Riverside, Riverside, CA 92521, USA
*Correspondence: xuan.liu@ucr.edu
http://dx.doi.org/10.1016/j.molcel.2013.10.031

SUMMARY

While p53 activation has long been studied, the mechanisms by which its targets genes are restored to their preactivation state are less clear. We report here that TAF1 phosphorylates p53 at Thr55, leading to dissociation of p53 from the p21 promoter and inactivation of transcription late in the DNA damage response. We further show that cellular ATP level might act as a molecular switch for Thr55 phosphorylation on the p21 promoter, indicating that TAF1 is a cellular ATP sensor. Upon DNA damage, cells undergo PARP-1-dependent ATP depletion, which is correlated with reduced TAF1 kinase activity and Thr55 phosphorylation, resulting in p21 activation. As cellular ATP levels recover, TAF1 is able to phosphorylate p53 on Thr55, which leads to dissociation of p53 from the p21 promoter. ChIP-sequencing analysis reveals p53 dissociates from promoters genome wide as cells recover from DNA damage, suggesting the general nature of this mechanism.

INTRODUCTION

The p53 tumor suppressor plays a critical role in the cellular response to DNA damage (Vousden and Prives, 2009; Kruse and Gu, 2009). The biochemical activity of p53 that is required for this role primarily relies on its ability to bind to specific DNA sequences and to control the transcription of its target genes. Among the genes induced by p53 is p21, which binds and inhibits all currently known cyclin-dependent protein kinases required for the G1-to-S phase transition. Upon DNA damage, the transcription activity of p53 is regulated through multiple posttranslational modifications (Bode and Dong, 2004; Kruse and Gu, 2009), including the phosphorylation of serine or threonine residues and the acetylation of lysine residues.

We have previously reported that p53 is phosphorylated by TAF1 at Thr55 and that this phosphorylation leads to p53 inactivation (Li et al., 2004; Cai and Liu, 2008). TAF1 is the largest subunit of transcription factor TFIID, which is composed of the TATA binding protein (TBP) and 13 to 14 TBP-associated factors (TAFs)(Burley and Roeder, 1996; Tora, 2002; Thomas and Chiang, 2006). In addition to its intrinsic protein kinase activity (Dikstein et al., 1996), TAF1 also contains a tandem pair of 110-residue motifs known as double-bromodomain (DBrD) modules (Jacobson et al., 2000). Interestingly, we also show that p53 recruits TAF1 to the p21 promoter through interaction between its acetyllysines and TAF1 DBrD and that this recruitment contributes to p53 activation (Li et al., 2007a). These data imply that TAF1 plays a dual role in regulation of p53. Perhaps at a later time of DNA damage, TAF1 may mark p53 for inactivation via Thr55 phosphorylation on the p21 promoter, thus inactivating p53-mediated transcription.

One conspicuous alteration during DNA damage, which may potentially allow TAF1 to play a dual role in p53 regulation, is cellular ATP levels. Upon DNA damage, cellular ATP is depleted by activated poly(ADP-ribose) polymerase-1 (PARP-1). PARP-1 is a nuclear enzyme that catalyzes the covalent attachment of ADP-ribose units on the γ-carboxyl group of Glu residues of acceptor proteins. This leads to modification of numerous proteins using NAD+ as a substrate and to exhaustion of cellular ATP (Schreiber et al., 2006). Of the ~18 predicted PARPs in the human genome (Amé et al., 2004), PARP-1 and PARP-2 are highly activated in response to DNA damage, with PARP-1 being responsible for about 90% of the activity. As a consequence, ATP has been reported depleted in wild-type, but not *PARP-1*$^{-/-}$ MEF cells, following DNA damage (Ha and Snyder, 1999). The altered ATP levels may potentially affect the dynamics of TAF1 phosphorylation, thus allowing it to function to both activate and terminate p53-mediated transcription.

To investigate this possibility, we first study whether TAF1 might phosphorylate p53 on the p21 promoter. By using an immobilized template DNA system, we show TAF1 phosphorylates p53 at Thr55 on the p21 promoter in a manner that is particularly sensitive to ATP levels, and this phosphorylation leads to p53 dissociation from the promoter. Importantly, we show that cellular or local ATP concentration fluctuations might act as a molecular switch for Thr55 phosphorylation on the p21 promoter, and this phosphorylation leads to inactivation of p21 transcription as cells recover from DNA damage. To assess the overall effect of the regulation, we performed chromatin immunoprecipitation sequencing (ChIP-seq) analysis and revealed p53 undergoes promoter dissociation at a global level as ATP levels recover from DNA damage. These data provide evidence for regulation of p53 transcription activity by cellular ATP levels and suggest molecular insights into inactivation of p53 transcription late in the DNA damage response.

RESULTS

Thr55 Phosphorylation by TAF1 Occurs on the p21 Promoter and Displaces p53 from the Promoter

We showed previously that p53 binds to an immobilized p21 promoter and recruits TAF1 to the promoter (Li et al., 2007a). We thus assessed whether TAF1 could directly phosphorylate p53 at Thr55 on the promoter using this immobilized template DNA system. After forming the immobilized p21 promoter-p53-TAF1 complex on Dynabeads, either ATP or a nonhydrolyzable ATP analog, ATP-γ-S, was added to the system. Subsequently, the beads with immobilized promoter complex and the flowthrough fractions were collected and analyzed (Figure 1A). The assay shows that p53 recruits TAF1 to the promoter, and, importantly, addition of ATP but not ATP-γ-S leads to a phosphorylation-dependent dissociation of p53 from the immobilized promoter (Figure 1B). Since the p53-TAF1 complex was preassembled on the promoter before adding ATP, this result indicates that TAF1 phosphorylation occurred on the promoter and promoted p53 dissociation from the promoter.

To investigate whether p53 dissociation was mediated through TAF1-mediated Thr55 phosphorylation, we substituted the p53 phosphorylation-defect mutant T55A in the system. As shown in Figure 1C, T55A could bind the immobilized p21 promoter and recruit TAF1; however, upon addition of ATP, both T55A and TAF1 remain bound to the promoter. Further, purified Thr55-phosphorylation-enriched p53 (Li et al., 2007b) binds to DNA with significantly lower affinity than nonphosphorylated protein in electrophoretic mobility shift assay (Figure S1 available online), and addition of the TAF1 kinase inhibitor apigenin (Li et al., 2004) restores both wild-type p53 and TAF1 retention on the immobilized p21 promoter (Figure 1D). These data suggest that TAF1 phosphorylates p53 at Thr55 on the p21 promoter, leading to p53 dissociation from the promoter.

To better mimic in vivo conditions, we used purified TFIID (Liu and Berk, 1995) to substitute TAF1 and conducted the assay in a range of ATP concentrations, including physiological levels in the cell (1–5 mM) (Gribble et al., 2000). As shown in Figure 1E, both p53 and T55A recruit TFIID complex to the promoter; however, addition of ATP only leads to dissociation of wild-type p53, but not T55A, from the promoter. Interestingly, both p53 phosphorylation and dissociation are ATP concentration dependent, indicating that cellular or local ATP level potentially could act as a molecular switch for p53 Thr55 phosphorylation and binding to the p21 promoter.

DNA Damage Induces Fluctuation of Cellular ATP Levels through PARP-1 and AMPK

To test this hypothesis, we first assessed cellular ATP fluctuation upon DNA damage. By comparing to a standard dilution curve of ATP and applying a volume of 4 pl per cell (Beck et al., 2011), the cellular ATP concentration was calculated as 1.13 ± 0.01 mM in U2OS cells. Treating U2OS cells with UV reduced cellular ATP level at earlier times (1.5–6 hr) and elevated it at later times (12–16 hr) (Figure 2A). To firmly establish this cellular ATP fluctuation, we showed that ATP-to-ADP ratio also reduced at earlier times and increased at later times after DNA damage (Figure 2B). Furthermore, similar trends of the ATP fluctuation are observed in H549, MCF7, and HCT116 cells (data not shown). We next tested whether activation of PARP-1 might play a role in early reduction of ATP levels upon DNA damage by treating U2OS cells with the PARP-1 inhibitors 4-amino-1, 8-naphthalimide (4-AN) (Horton et al., 2005), or 8-hydroxy-2-methylquinazolin-4-one (NU1025; Boulton et al., 1999). The efficient prevention of PARP-1 activation and resultant cellular ATP reduction were indeed evident upon PARP-1 inhibition (Figures 2A, 2C and S2A). The protein levels of PARP-1 were not affected (Figure 2E). Because DNA double-strand breaks (DSBs) were a prime cause of PARP-1 activation, we treated cells with bleomycin, a DNA-damaging alkylating agent that generates DSBs with high specificity (Dong et al., 2010), and confirmed the role of PARP-1 activation in reduction of ATP level upon DNA damage (Figures 2D and S2B).

Reduction of cellular ATP levels will inevitably lead to cellular AMP-to-ATP ratio increase, and thereby activation of AMP-activated protein kinase (AMPK). Once activated, AMPK leads to several metabolic responses (Hardie, 2007) that could elevate ATP levels at later times of DNA damage. In fact, a recent paper has suggested that PARP1-mediated ATP depletion activated AMPK in HEK293 cells (Ethier et al., 2012). To test this possibility, we assayed AMPK activity using either phosphoThr172-specific antibody or an AMPK assay kit (Figures 2E and S2C). Activation of AMPK was clearly detected at later times of DNA damage (UV or bleomycin), and, notably, treating cells with 4-AN completely blocks this activation. Further, treating cells with the AMPK inhibitor, Compound C (Zhou et al., 2001; Figures 2F and S2C), or overexpression of a dominant-negative mutant of AMPK (DN-AMPK) (Inoki et al., 2003; Figure S2D) blocked elevation of ATP levels at later times of DNA damage. Together these results suggest that PARP-1-mediated ATP reduction occurs at earlier times of DNA damage, which results in AMPK activation and ATP increase at later times of DNA damage.

Fluctuations in Cellular ATP Correlate TAF1 Activity

Next, we investigated the effect of cellular ATP on p53 Thr55 phosphorylation. As shown in Figure 3A, increased Thr55 phosphorylation, but not other phosphorylation, was indeed detected at 12 and 16 hr after DNA damage. Notably, we also detected a decreased Thr55 phosphorylation at 2 hr after DNA damage. This is likely due to the combinatory effect of lower cellular ATP level and activation of PP2A (Li et al., 2007b). Significantly, treating cells with either 4-AN (Figure 3A), Compound C (Figures 3A and S2C), or DN-AMPK (Figure S2D) effectively blocked increased Thr55 phosphorylation. To exclude the possibility that AMPK may phosphorylate and activate TAF1 under our assay conditions, we show activation of AMPK by AICAR (Narkar et al., 2008), an AMP analog that leads to phosphorylation of acetyl-CoA carboxylase (a known AMPK substrate), did not affect TAF1-mediated Thr55 phosphorylation (Figure S3A). To ensure that cellular ATP level indeed affects p53 Thr55 phosphorylation, we show that treating cells with high glucose, which elevates cellular ATP levels, also increased p53 Thr55 (but not other) phosphorylation (Figure S3B). Together, our data suggest that, upon DNA damage, cellular ATP level fluctuates, which modulates p53 Thr55 phosphorylation.

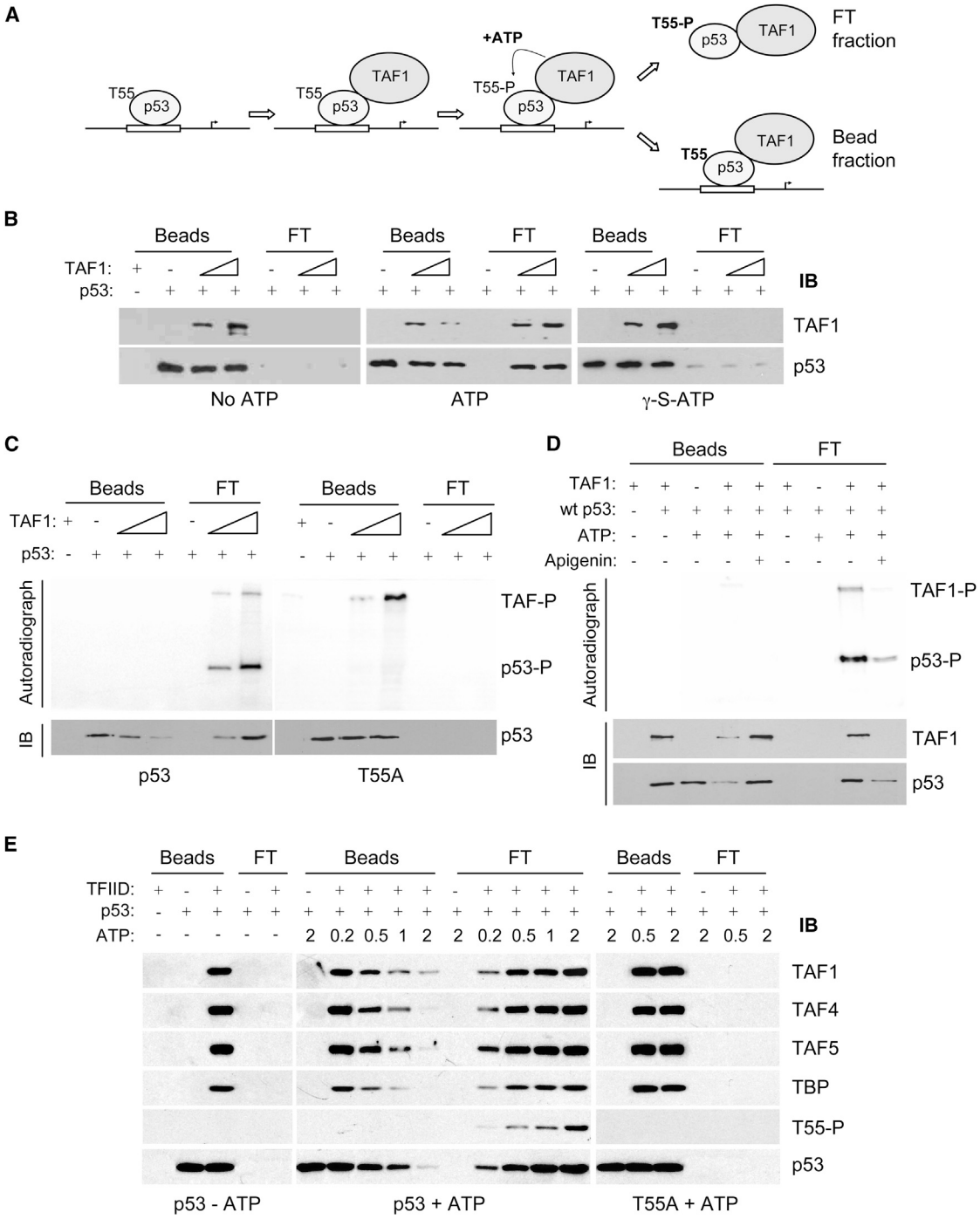

Figure 1. Thr55 Phosphorylation by TAF1 Occurs on the Immobilized p21 Promoter and Displaces p53 from the Promoter

(A) Schematic representation of preassembly of p53-TAF1 complex and phosphorylation of p53 by TAF1 on immobilized p21 promoter.

(B) ATP or ATP-γ-S was added to preassembled p53-TAF1 complex on the p21 promoter. Following phosphorylation, immobilized promoter and flowthrough fractions were separated and assayed for p53 and TAF1 by immunoblotting.

(C) Preassembled p53-TAF1 promoter or T55A-TAF1 promoter was subjected to phosphorylation assay in the presence of ^{32}P-γ-ATP, separated to immobilized bead and flowthrough fractions, and analyzed with autoradiograph or p53 immunoblotting.

(D) Preassembled p53-TAF1 promoter was subjected to phosphorylation assay in the absence or presence of apigenin.

(E) Affinity-purified TFIID and p53 were preassembled on the p21 promoter, and phosphorylation assays were carried out at a range of ATP concentrations, as indicated. The immobilized promoter and flowthrough fractions were separated and analyzed for TAF1, TAF4, TAF5, TBP, Thr55-Phos, and p53 by immunoblotting. See also Figure S1.

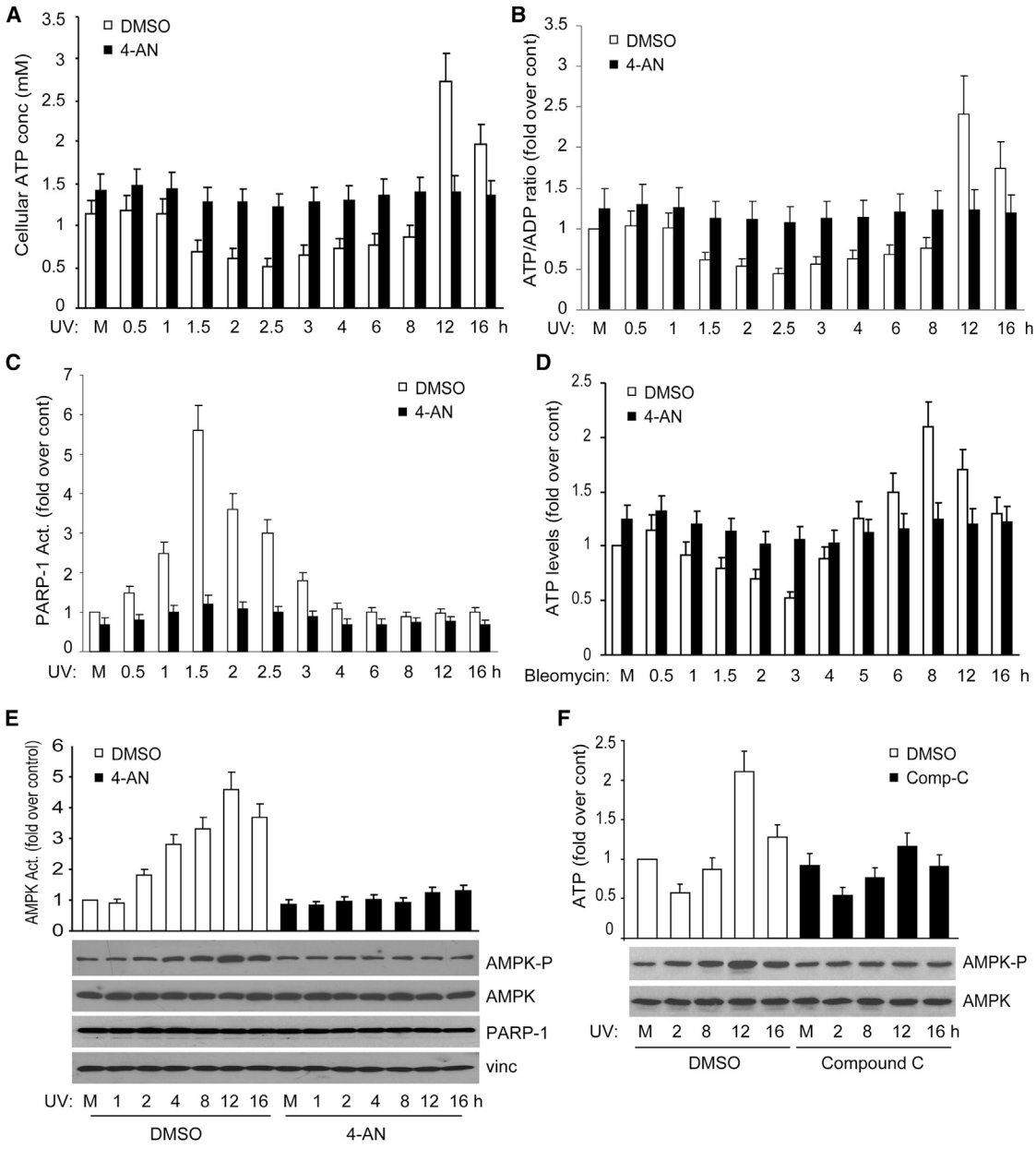

Figure 2. DNA Damage Induces Fluctuation of Cellular ATP Levels through PARP-1 and AMPK

(A–D) U2OS cells were either untreated (M) or subjected to DNA damage in the presence or absence of 4-AN, and cell lysates were collected at the time points indicated. (A and D) Cellular ATP levels were determined using a luciferin/luciferase method according to manufacturer's protocol. The initial values of ATP levels were 4.54 nmol per 1×10^6 cells, with a cellular concentration of 1.1 mM. Bars represent average of triplicate experiments ± SD.

(B) Cellular ATP/ADP ratio was assayed at the time points indicated, and bars represent average of triplicate experiments ± SD.

(C) PARP-1 activity was measured using a PARP-1 detection kit according to manufacturer's protocol. Bars represent average of triplicate experiments ± SD.

(E and F) Cell lysates were subjected to immunoblotting for each of the proteins as indicated. The activity of AMPK was also assayed using an AMPK activity assay kit according to manufacturer's protocol in (E). The results are presented as fold (mean ± SE) over untreated cells (M) from three independent experiments. See also Figure S2.

To further support this view, we assessed whether cellular ATP fluctuation could directly affect TAF1 kinase activity in an in vitro phosphorylation reaction using TAF1 immunoprecipitated from cells as kinase and affinity-purified p53 as substrate. As shown in Figure 3B, TAF1 immunoprecipitated from mock-treated U2OS cells displays a low but specific autophosphorylation, as well as p53 Thr55 phosphorylation. Both signals, however, were significantly enhanced when TAF1 was purified from 12 hr UV-treated cells. Importantly, inhibition of AMPK with either Compound C (Figure 3B) or DN-AMPK (Figure S3D) completely

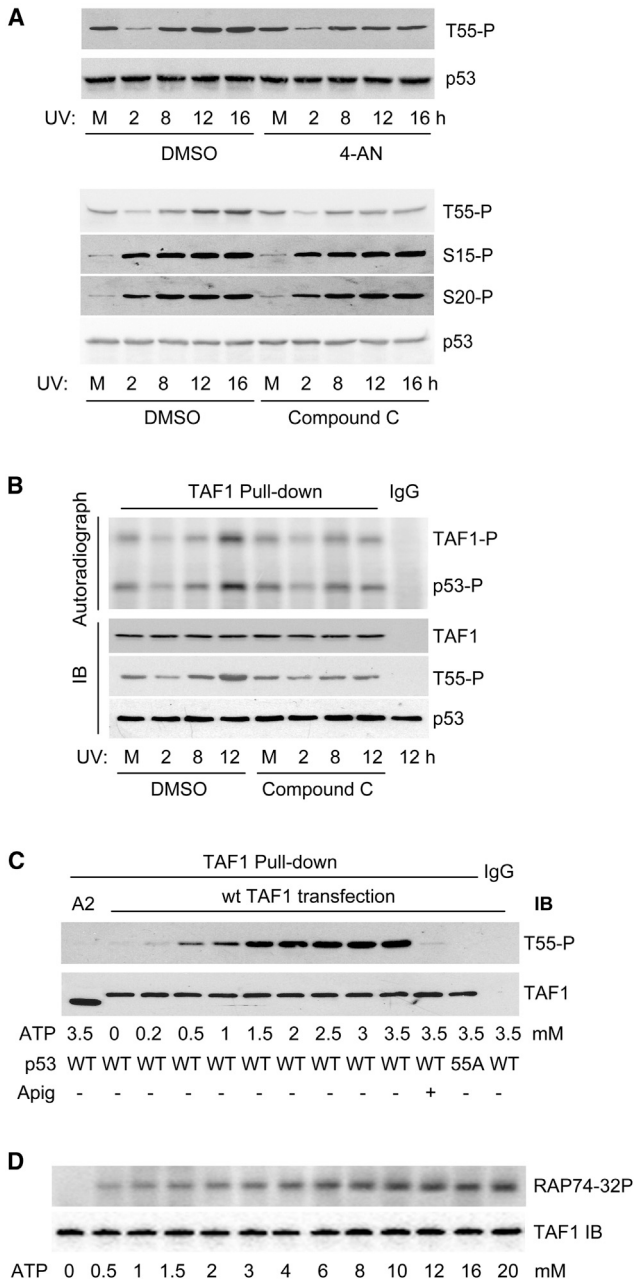

Figure 3. TAF1 Kinase Activity and p53 Thr55 Phosphorylation Are Sensitive to Fluctuations in Cellular ATP Levels

(A and B) U2OS cells, pretreated with MG132 to normalize p53 protein levels, were either untreated (M) or subjected to UV irradiation, and cell lysates were collected at the time points indicated.

(A) Cell lysates were subjected to immunoblotting for p53 phosphorylation, as indicated.

(B) Nuclear extracts were immunoprecipitated with anti-TAF1 antibody Ab1230 at the time points indicated. In vitro phosphorylation assay was carried out using immunoprecipitated TAF1 and purified p53. TAF1 and p53 phosphorylation were detected by either autoradiograph or immunoblotting, as indicated.

(C and D) Nuclear extract from U2OS cells that were transfected with either wild-type HA-TAF1 or the A2 mutant were immunoprecipitated with HA antibody, and in vitro phosphorylation assay was carried out with purified p53 or RAP74 in the presence of various ATP concentrations. See also Figure S3.

blocked enhanced TAF1 kinase activity. To provide direct evidence for regulation of TAF1 kinase activity by ATP, we immunoprecipitated TAF1 from U2OS cells transfected with either wild-type TAF1 or kinase-dead A2 mutant (O'Brien and Tjian, 1998) and subjected them to in vitro p53 phosphorylation (Figure 3C) in the presence of a range of ATP concentrations. The assay showed higher specific activity of TAF1 upon increasing ATP concentrations, whereas the A2 mutant or inhibition of TAF1 by apigenin did not lead to p53 phosphorylation. To exclude the possibility that ATP concentrations in the reaction might be affected by contaminant activities, we showed that ATP levels were largely unchanged in the presence of the TAF1 inhibitor apigenin (Figure S3C). Similarly, phosphorylation of RAP74, another substrate of TAF1 (Dikstein et al., 1996), by TAF1 was also enhanced by increased ATP concentrations (Figure 3D). On the basis of these results, we calculated K_m for ATP ($K_{m,\ ATP}$) of 1.9 mM for TAF1. Consistent with the notion that ATM has $K_{m,\ ATP}$ of 29 μM (Knight and Shokat, 2005), ATM-mediated p53 Ser15 phosphorylation was not affected by the same range of ATP concentrations (Figure S3E). These results suggest that TAF1 may function as an ATP sensor in the cell, allowing response to cellular or local ATP fluctuation. In addition, our data also provided further evidence for TAF1-mediated p53 Thr55 phosphorylation at later times of DNA damage.

TAF1-Mediated Thr55 Phosphorylation Leads to Dissociation of p53 from the p21 Promoter after DNA Damage

Next, we investigated whether increased Thr55 phosphorylation leads to dissociation of p53 from the p21 promoter at later times of DNA damage by ChIP approach (Figure 4A). Consistent with our previous finding (Li et al., 2007a), increased p53 binding to the 5′ and 3′ p53-binding sites, as well as to the proximal core promoter region (pp) on the p21 promoter, was detected at 2 and 8 hr after DNA damage. Further, increased TAF1, TAF4, and TAF5 binding to the 3′ site, as well as to the pp of the p21 promoter, was also detected. At 12 and 16 hr after DNA damage while cellular ATP levels were elevated, however, the p53 binding to all three regions on the p21 promoter was significantly reduced (33% at the 5′ binding site and 22% at the 3′ binding site and core promoter, as quantitated by ChIP-qPCR; Figure S4A). Importantly, the bindings of TAF1, TAF4, and TAF5 to the promoter were also reduced concurrently (Figure 4A). Although dissociation of TBP was detected at the 3′ p53-binding site, it remains bound on the core promoter region at later times of DNA damage. Because TBP is also detected on the core promoter before DNA damage, this result suggests that TBP is likely to bind or crosslink to the core promoter region distinctively from TAFs.

To confirm the role of ATP levels on p53 DNA binding, we show treating cells with the PARP-1 inhibitor 4-AN prevents the dissociation of p53 and TAFs from the p21 promoter (Figure 4A). Further, inhibition of AMPK activation with either Compound C (Figure 4A) or DN-AMPK (Figure S4B) also effectively prevents the dissociation. Finally, treating cells with the TAF1 kinase inhibitor apigenin also abolishes the dissociation (Figure 4A). To ensure the p53 dissociation is not specific for UV irradiation, we showed that treating cells with bleomycin also dissociated

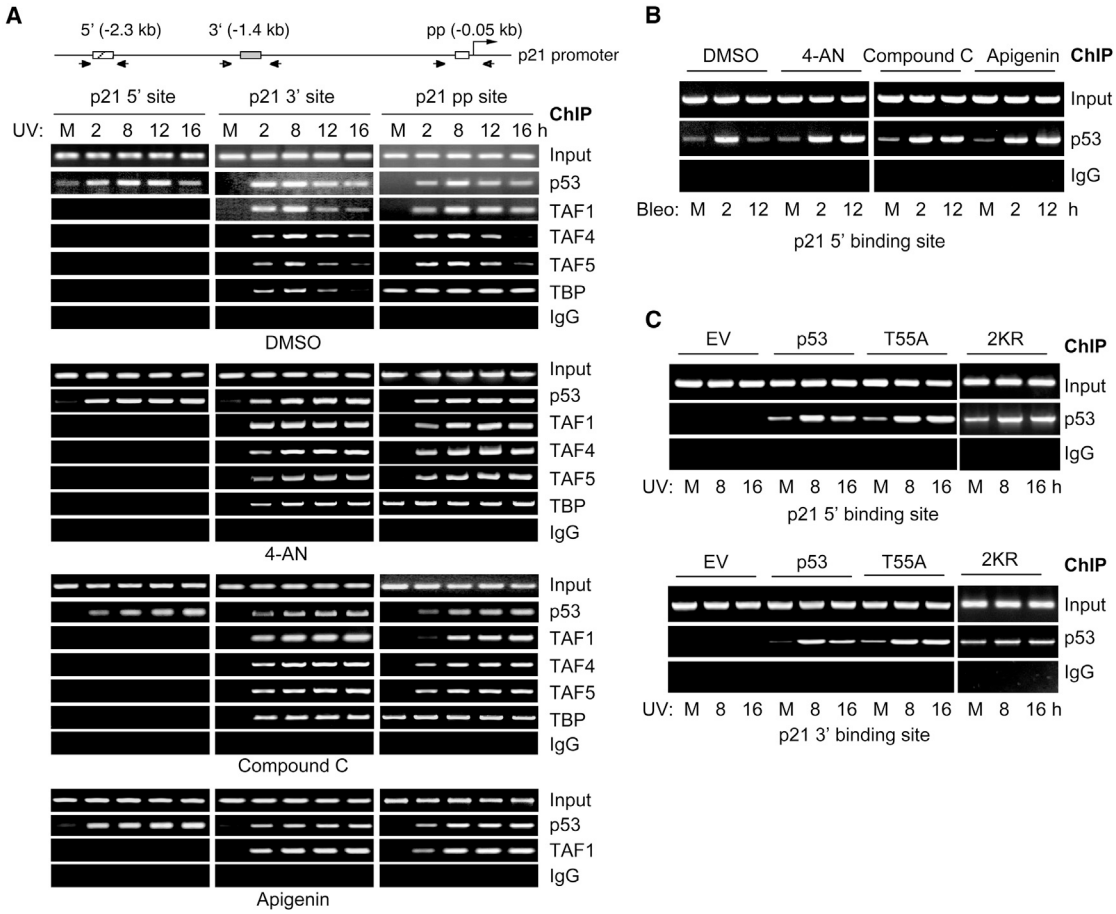

Figure 4. TAF1-Mediated Thr55 Phosphorylation Leads to Dissociation of p53 from the p21 Promoter Late in the DNA Damage Response

(A) U2OS cells were either untreated (M) or subjected to UV irradiation in the absence or presence of 4-AN, Compound C, or apigenin, and ChIP analysis of the p21 promoter was assayed at the time points indicated. Binding sites that were amplified by PCR are indicated on the top of each panel. Antibodies used in ChIP are listed on the right. PCR products were resolved by agarose gel electrophoresis and visualized by ethidium bromide staining.

(B) U2OS cells were treated with bleomycin in the absence or presence of 4-AN, Compound C, or apigenin, and ChIP analysis was assayed at the time points indicated.

(C) HCT116 $p53^{-/-}$ cells were transfected with wild-type p53, T55A, or 2KR; either untreated (M) or subjected to UV irradiation; and ChIP analysis was assayed at the time points indicated. See also Figure S4.

p53 from the p21 promoter at later times and, importantly, addition of 4-AN, Compound C, or apigenin blocks the dissociation (Figure 4B). To firmly establish the role of Thr55 phosphorylation in the dissociation of p53 from the promoter, we compared the ability of wild-type p53 and T55A to bind to the p21 promoter at 8 and 16 hr after DNA damage. As shown in Figure 4C, bindings of p53 to both p53-binding sites (3′ and 5′) on the p21 promoter were significantly reduced at 16 hr after DNA damage, whereas binding of T55A remained unchanged. These data suggest that increased ATP level enhances TAF1-mediated p53 Thr55 phosphorylation on the p21 promoter, resulting in dissociation of p53 and TFIID from the promoter.

Genome-wide Analysis Reveals an Overall Dissociation of p53 from Promoters after DNA Damage

To investigate the effect of cellular ATP on overall p53 DNA binding, we first employed ChIP-seq approach to assess genome wide p53 occupancy at 0, 8, and 16 hr after DNA damage. We identified 97, 838, and 689 chromatin regions with significant p53 enrichments above the input background at 0, 8, and 16 hr after DNA damage (Figure S5B; Table S1). Analysis of the identified chromatin regions reveals that p53 binding was enriched near the transcription start sites (TSSs) in response to DNA damage (Figure S5A). Importantly, the most enriched motif identifiable at sites bound by p53 was indeed the well-characterized p53-binding motif at all three time points (Figure 5A).

Among the total p53-bound chromatin regions at 8 hr after DNA damage, 830 of them (including *p21*) exhibited stronger p53 occupancy (2-fold or more) as compared to those observed before DNA damage (0 hr), suggesting that p53 binding to those chromatin regions was induced upon UV (Figure S5B; Table S2). Functional annotation analyses of those chromatin regions revealed a striking enrichment of the p53 signaling pathway (23 folds) and enrichment of p53 on genes with functions in stress

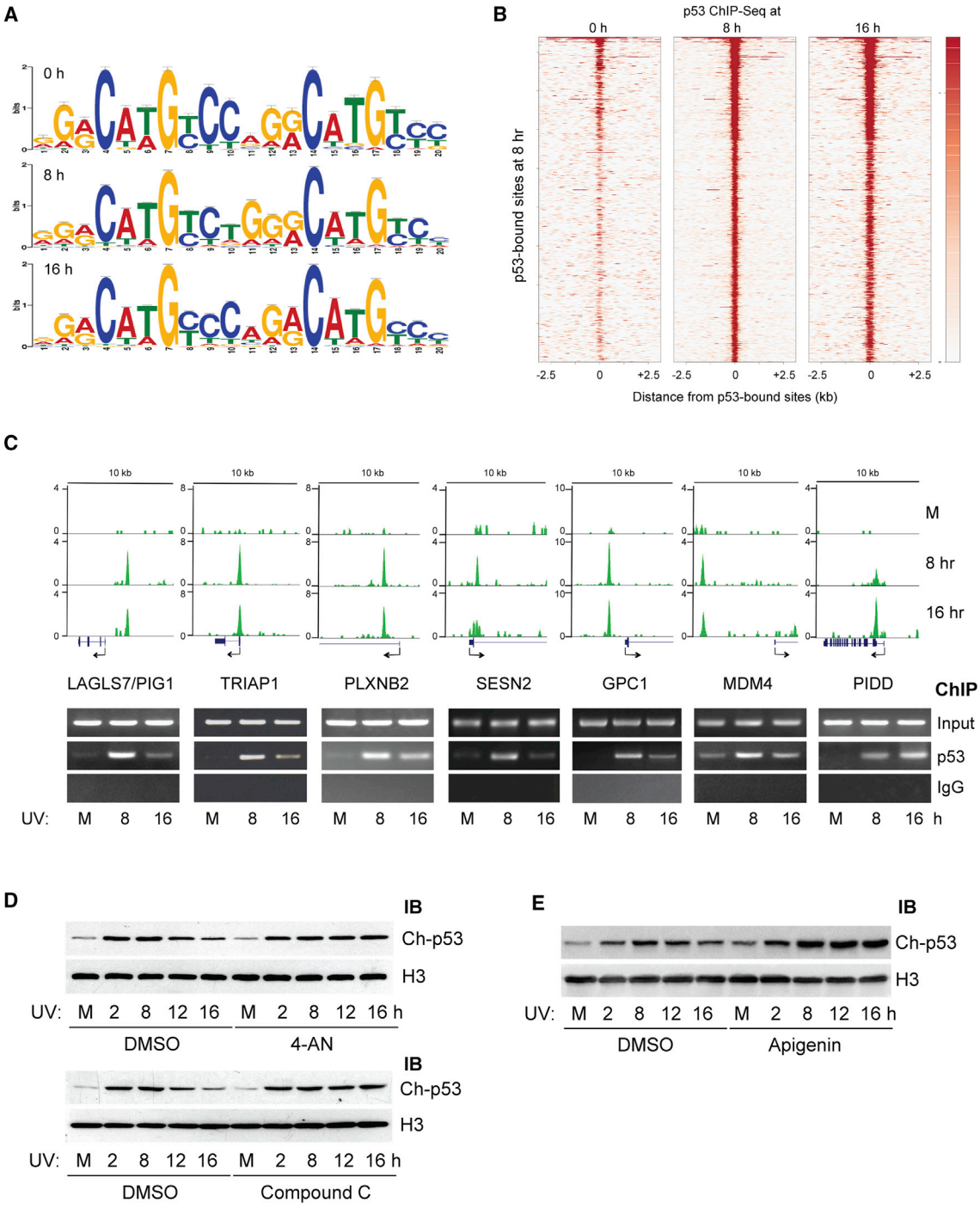

Figure 5. Genome-wide Analysis Reveals p53 Dissociation from Its Target Promoters Late in the DNA Damage Response

(A) p53-binding motif found enriched at 0 hr (top), 8 hr (middle), and 16 hr (bottom) after DNA damage.

(B) Heatmaps showing p53 ChIP-seq levels of 5 kb regions centered on the summit of the peaks at 0 hr (left), 8 hr (middle), and 16 hr (right). The heatmap is ranked according to the enrichment of p53 occupancy at 8 hr after DNA damage. (Red represents enriched; white represents not enriched).

(C) Individual gene tracks of p53 binding at the LAGLS, TRIAP1, PLXNB2, SESN2, GPC1, MDM4, and PIDD promoters at 0 hr (top), 8 hr (middle), and 16 hr (bottom) after DNA damage. The x axis shows genomic position. The y axis shows signal per million reads for fragment pileup profiles generated by MACS2. Verification of p53 binding on the corresponding genes by individual ChIP was shown below.

(D and E) U2OS cells were treated with control (DMSO), the PARP-1 inhibitor 4-AN, the AMPK inhibitor Compound C, or the TAF1 kinase inhibitor apigenin; either untreated (M) or subjected to UV irradiation; fractionated to chromatin-bound and unbound fractions; and analyzed for p53 and histone H3 protein levels by immunoblotting of chromatin-bound fraction. See also Figure S5.

response, apoptosis, and cell-cycle arrest (Figure S5C). Significantly, of the total 830 p53-bound chromatin regions, 340 of them (also including *p21*) showed reduced p53 occupancy (2-fold or more) at 16 hr after DNA damage (Figure S5B; Table S2), indicating an extensive reduction of p53 DNA binding at 16 hr after DNA damage (Figure 5B).

To verify the ChIP-seq results, we used individual ChIP assay to analyze p53 binding on seven of its target genes, six of which (*LGALS7*, *TRIAP1*, *PLXNB2*, *SESN2*, *GPC1*, and *MDM4*) displayed increased p53 binding at 8 hr and reduced binding at 16 hr after DNA damage and one of which (*PIDD*) displayed increased p53 binding at 8 hr, but no reduced binding at 16 hr (Figure 5C). The assay shows that p53 bindings detected by individual ChIP assay on all seven genes are consistent with those obtained by ChIP-seq (Figure 5C). Together, our data suggest that p53 undergoes promoter dissociation from its target genes at a global level at 16 hr after DNA damage.

To provide evidence for the effect of cellular ATP on overall p53 dissociation from DNA, we treated cells with UV and subjected them to subcellular fractionation to obtain chromatin-bound p53 fraction (Li et al., 2007a). Consistent with our ChIP-seq results, the relative amount of p53 in chromatin-bound fraction increases at earlier times (2–8 hr) and reduces at later times (12–16 hr) after DNA damage (Figure 5D). Importantly, inhibition of PARP-1 and AMPK effectively eliminates the reduction at later times after DNA damage (Figures 5D and S5D). Treating cells with the TAF1 kinase inhibitor apigenin also abolishes the reduction (Figure 5E).

TAF1-Mediated Thr55 Phosphorylation Leads to Inactivation of p53 Transcription

Our finding that Thr55 phosphorylation leads to dissociation of p53 and TFIID from the promoter prompts us to test its role in inactivation of p53 transcription. We conducted RT-PCR assay at corresponding time points after UV irradiation and observed p21 mRNA levels increase at earlier times and decrease at later times after DNA damage (Figure 6A). To exclude the possibility that RNA stability or splicing might have caused mRNA level change, we also conducted RT-PCR assay to amplify a region of p21 heterogeneous nuclear RNA (hnRNA) transcript and showed p21 hnRNA levels were also reduced at the corresponding times (Figure 6A). All hnRNA analyses are quantitated by RT-qPCR (Figure 6A). Reduction of LGALS7/PIG1 (p53-induced gene 1) was also detected at corresponding times (Figures 6A and S6B), suggesting a broader role of this mechanism of inactivation of transcription at other p53 target genes. Further, treating cells with PARP-1, AMPK, or TAF1 inhibitor completely blocks the reduction of p21 and PIG1 transcripts at later times of DNA damage (Figures 6A and S6A). Similar results were also observed in HCT116 $p53^{+/+}$ cells (Figure S6C).

We next investigated biological significance of the regulation. As shown in Figure 6B, UV treatment alone causes 21.1% of cells to undergo apoptosis. The combination of UV with either the AMPK inhibitor, Compound C, or the PARP-1 inhibitor, 4-AN, led to increases in cell apoptosis (38.1% or 43.27%, respectively), while treating cells with those inhibitors alone had no effect. Similarly, treating cells with Compound C or 4-AN also enhanced bleomycin-induced cell apoptosis (Figure S6D). Furthermore, T55A indeed showed higher apoptotic activity than wild-type p53 (Figure S6E).

DISCUSSION

Current views of transcription regulation place most of their focus on the events that precede initiation of transcription. Although these events play a crucial role in regulating gene expression, correct regulation also requires turning off transcription when no longer needed. Because a DNA-bound activator interacts and recruits components of the basal transcription apparatus to the promoter, signaling transcription initiation, one or more of those basal factors could, in theory, mark the transcription activator, presumably through posttranslational modification after transcription, leading to cessation of transcription. In our previous study, we showed that acetylated p53 at K373 and K382 induces p21 transcription through interacting with TAF1 DBrD (Li et al., 2007a). This unique interaction is probably important for keeping TAF1 in a close proximity to p53, allowing Thr55 phosphorylation to occur on the promoter and turn off p21 transcription. Our result that the p53 acetylation mutants that fail to bind to TAF1 also fail to be phosphorylated by TAF1 (Figure 7) and dissociated from the p21 promoter (Figure 4C) supports this view. Because inactivation of p53 on promoters after responding to DNA damage has not been well studied before, our findings provided additional insights into the regulation of p53-mediated transcription. Furthermore, because TAF1 is a component of general transcription machinery bound to many promoters (Kim et al., 2005), our results may provide important clues about promoter inactivation in general.

It is clear that that nutrient availability is likely sensed at multiple levels in mammalian cells. For example, AMPK is activated in response to ATP depletion and/or AMP accumulation (Hardie, 2007). Mammalian target of rapamycin is activated in a manner dependent on cellular amino acid levels (Guertin and Sabatini, 2009) and ATP levels (Dennis et al., 2001). Because TAF1 is a cell-cycle regulatory protein important for G1 progression (Sekiguchi et al., 1991; Wang and Tjian, 1994; Li et al., 2004), its ability to sense cellular ATP may be critical for instructing cells, at transcription level, as to whether available nutrients/ATP are sufficient to permit cell growth. Indeed, our ChIP-seq analysis reveals activation of several p53-mediated cell growth arrest genes (such as *p21* and *SESN2*) is reduced upon ATP-dependent TAF1 phosphorylation. However, our ChIP-seq analysis also reveals reduction of p53 activation of apoptosis genes (such as *PIG1*) and metabolism genes (such as *TIGAR*; Table S2) at 16 hr after DNA damage, suggesting ATP-dependent TAF1 phosphorylation may inhibit overall p53 tumor suppressor activity. Interestingly, metabolic stress has been shown to activate p53 through AMPK-mediated Ser15 phosphorylation (Jones et al., 2005), suggesting that nutritional status could regulate p53 transcription activity through multiple pathways. Upon metabolic stress (or lower cellular ATP levels), p53 is activated by AMPK phosphorylation, so cells can undergo stress-mediated G1 arrest. In nutrition-rich conditions (or higher cellular ATP levels), however, p53 is inactivated by ATP-dependent TAF1 phosphorylation, so cells can undergo G1 progression. Finally, although metabolic alterations have been linked to

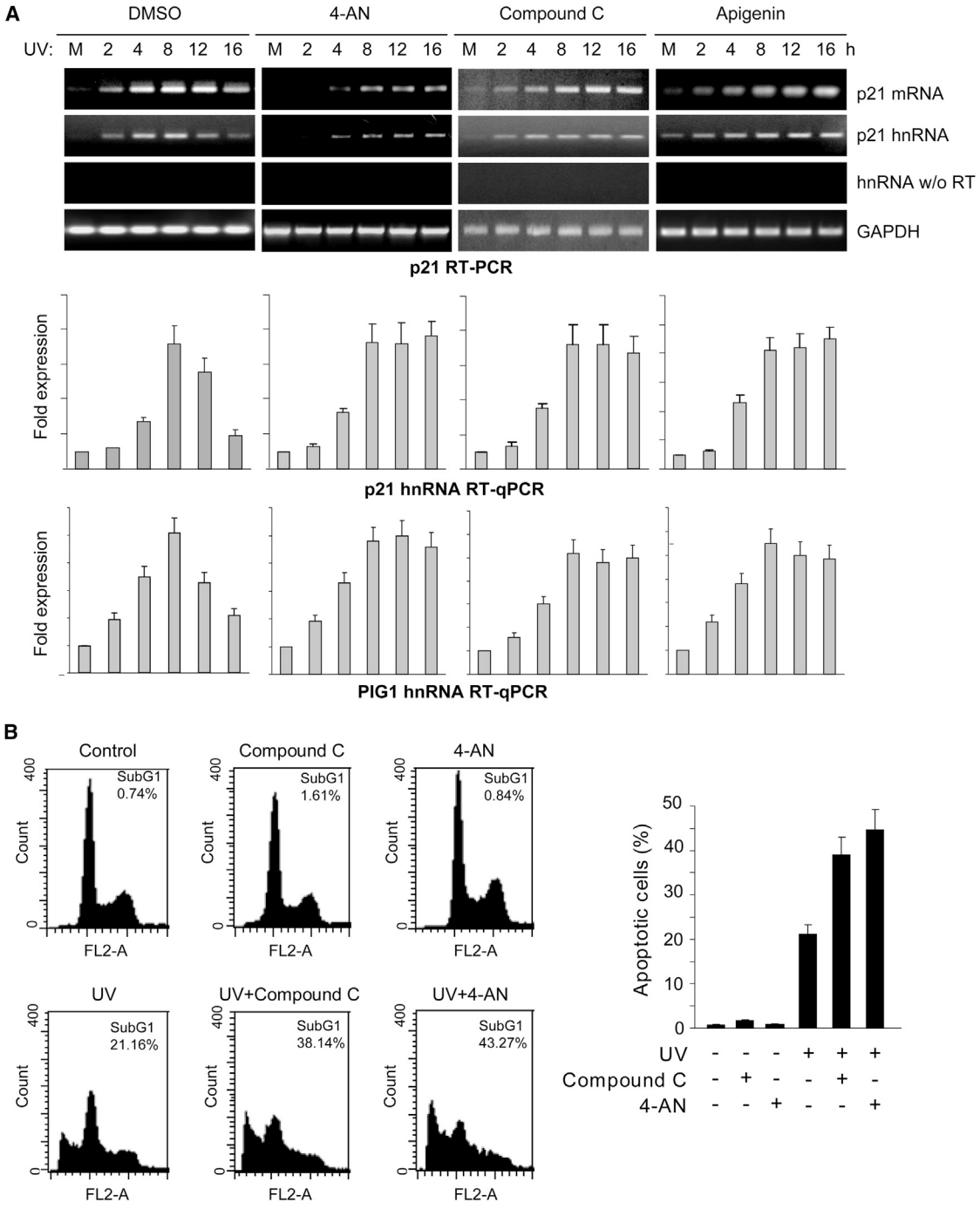

Figure 6. TAF1-Mediated Thr55 Phosphorylation Leads to Inactivation of Transcription of p53 Target Genes

(A) U2OS cells were treated with control (DMSO), 4-AN, Compound C, or apigenin, and then either untreated (M) or subjected to UV irradiation. The p21 mRNA and prespliced RNA (hnRNA), as well as PIG1 hnRNA levels for each treatment, were analyzed by either RT-PCR or RT-qPCR at the time points indicated. All hnRNA are normalized to GAPDH and presented as fold (mean ± SE) over untreated cells (M) based on three experiments.

(B) U2OS cells were treated with control, Compound C, or 4-AN; either untreated (control) or subjected to UV irradiation; and processed for FACS analysis for apoptotic cells (SubG1) according to DNA content. Apoptotic cells are presented as mean ± SE based on three independent experiments. See also Figure S6.

cancer for several decades (Warburg, 1956; Vander Heiden et al., 2009), little is known about how cellular metabolites affect p53 tumor suppressor function in cancer. Thus, our data that cellular ATP directly impacts its association with promoters provided evidence for regulation of p53-mediated transcription activation by cellular metabolites.

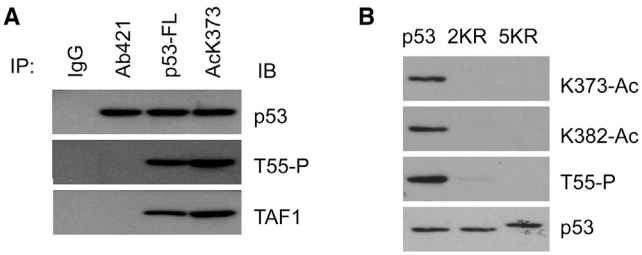

Figure 7. p53 Acetylation Is Required for Thr55 Phosphorylation

(A) p53 Thr55 phosphorylation was assayed by immunoprecipitation of cell lysates from U2OS cells with either K373 acetyl-specific, Ab421 (which binds to unacetylated p53), or p53-FL antibody, followed by immunoblotting with Thr55 phosphospecific antibody. The p53-TAF1 interaction was confirmed by immunoblotting with anti-TAF1 antibody.

(B) H1299 cells were transfected with wild-type p53, p53 acetylation mutant K373/382R (2KR), or K370/372/373/381/382 (5KR). p53 acetylation and Thr55 phosphorylation were detected using corresponding antibodies, as indicated.

EXPERIMENTAL PROCEDURES

Reagents and Western Blot Analysis

For DNA damage, U2OS and HCT116 *p53*$^{-/-}$ cells were subjected to UV radiation (20 J/m^2) or 30 μg/ml bleomycin (Sigma). For inhibition of PARP-1 activity, U2OS cells were treated with 1 μM 4-AN (Trevigen) 30 min before UV exposure. For inhibition of AMPK activity, U2OS cells were either treated with 10 μM Compound C (Calbiochem) 30 min before UV exposure or infected with a recombinant adenovirus expressing a DN-AMPK (Ad-DN-AMPK). For inhibition of TAF1, U2OS cells were treated with 40 μM apigenin (Sigma). Antibodies used in western blot analysis were anti-p53 (DO-1, Santa Cruz), anti-TAF1 (Ab1230), anti-TAF4 (Ab4A6, a gift of Dr. E. Wang), anti-TAF5 (a gift of Dr. R.G. Roeder), anti-TBP (SI-1, Santa Cruz), anti-TAF9 (C-19, Santa Cruz), anti-Thr55-Phos (Ab202), anti-vinculin (VIN-11-5, Sigma), anti-AMPK (Ab23A3, Cell Signaling Technology), anti-phospho-AMPK (40H9, Cell Signaling Technology), and anti-histone H3 (Ab24834, Abcam) antibodies.

Phosphorylation of p53 on Immobilized p21 Promoter

The p53, T55A, and TAF1 proteins were affinity purified as described (Li et al., 2004). TFIID was affinity purified from LTRα3 cells that express HA-tagged TBP (Liu and Berk, 1995). Binding of p53 and TAF1 or TFIID to immobilized p21 promoter (−2.4 kb to −0.15 kb) was conducted as described (Li et al., 2007a). Phosphorylation reactions were carried out by adding ATP in phosphorylation buffer (20 mM HEPES [pH 7.9], 12 mM $MgCl_2$, 100 mM KCl, 10% glycerol, 0.1 mM EDTA, and 1 mg/ml BSA) at 30°C for 15 min. Reaction mixtures were then separated into beads and flowthrough fractions, and the beads fractions were further washed with 100 mM KCl D buffer (20 mM HEPES [pH 7.9], 20% glycerol, 0.2 mM EDTA, 0.5 mM PMSF, and 0.5 mM DTT). The reaction mixtures from the beads or the flowthrough fractions were analyzed by SDS-PAGE for either autoradiography or immunoblotting.

Cellular ATP Level and ATP/ADP Ratio

ATP level was measured by the luciferin/luciferase method using the ATP Determination Kit according to manufacturer's protocol (Molecular Probes). Cellular ATP concentration was determined by comparing to a standard dilution curve of fresh ATP (Cell Signaling Technologies). The cell volume of 4 pl was used for calculation of cellular ATP concentration in U2OS cells, as reported in Beck et al. (2011). For measuring total ATP+ADP, ADP was first converted into ATP by mixing 2.3 units pyruvate kinase (Lee Biosolutions) to 100 μl cell lysate and incubating at room temperature for 15 min. ADP levels were then calculated by subtracting ATP from the total ATP+ADP. A standard curve was generated from known concentrations of ATP and ADP in each experiment and used to calculate the concentration of ATP and ADP in each sample. The results were expressed as fold (means ± SE) over untreated cells (mock) from three independent experiments.

PARP-1 Assay

The activity of PARP-1 was measured using a colorimetric assay for incorporation of biotinylated NAD (6-biotin-17-nicotinamide-adenine-dinucleotide) in a PAR primed at solid phase-immobilized histone H1 in the presence of activated DNA according to manufacturer's protocol (Trevigen). The measured PARP-1 activity was normalized by protein concentrations, and fold activation was calculated relative to the activity of untreated cells (mock). The results presented are the means ± SE of three independent experiments performed in duplicates.

TAF1 Kinase Assay

Nuclear extract was prepared from U2OS cells as described previously, and TAF1 was immunoprecipated with TAF1 antibodies (Ab1230), washed two times with ice-cold lysis buffer, two times with lysis buffer containing 500 mM NaCl, and two times with phosphorylation buffer. The following phosphatase and protease inhibitors were present throughout the purification: 1 mM Na_3VO_4, 1 mM NaF, 10 mM Na_2MoO_4, 20 mM β-glycerophosphate, 5 μM microcystin, 5 nM okadaic acid, 5 μg/ml aprotinin, 5 μg/ml leupeptin, and 5 μg/ml pepstatin, 1 mM PMSF, and 1 mM DTT. In vitro TAF1 phosphorylation assay was carried out using 120 ng of purified p53 as substrate with various concentrations of ATP in 20 μl of phosphorylation buffer under conditions as described (Li et al., 2004). For determining K_m for ATP, U2OS cells were transfected with either TAF1-expressing vector (pCMV-HAhTAF11) or A2/N7Ala-expressing vector (p-LXSN-MT-TAF1N1398 A2/N7Ala2) that expresses a kinase-dead TAF1 (A2), TAF1 was immunoprecipated with anti-HA antibodies, and phosphorylation was carried out for 20 min. Thr55 phosphorylation of p53 was detected by anti-Thr55-Phos antibody and phosphorylation of RAP74 was detected by autoradiography. K_m for ATP was analyzed using a nonlinear least-squares fitting of the data to a hyperbolic equation using PeakFit v4.01 (Jandel Scienfic).

ChIP Analysis

ChIP analysis was carried out as described previously (Li et al., 2007a). For U2OS and HCT116 *p53*$^{+/+}$ cells, nuclear extracts were collected at indicated time points after mock or 20 J/m^2 UVC treatment and sonicated to generate chromatin fragments of 500 bp. Antibodies and *p21* primer sets used in PCR were as described (Li et al., 2007a). Primer set for *LGALS7* are 5′-GTCC ACAAAAAGAAAAGACACTCCT and 5′-TACAGGAAAGGAGCCAGCCT; for *TRIAP1*, 5′-AGCTGTCCCCCTTGAGAAAT and 5′-GCGACCACATTTCTTC CTTC; for *PLXNB2*, 5′-CAACCTTGGGGCTTTCTCCA and 5′-GGCTGCCTG CCAAGAAAGA; for *SESN2*, 5′-CCTGGCCAATGAGGGAGAA and 5′-TGAG GTCGACTTTCACTGGC; for *GPC1*, 5′-ACCGTGCTGGATAAGGTGTG and 5′-GAAGGTTGCTCCTTCACCCA; for *MDM4*, 5′-TAAAAACTAGCCGGGTG TGG and 5′-TTCACACTTAGGGCCAGCTA; and for *PIDD*, 5′-CCGAATCCTCT GAAGCATCT and 5′-CTCTAGAGCTCCCCACTCCA. All binding sites were amplified with 30–35 cycles of PCR. The PCR products were electrophoresed by agarose gels and visualized by ethidium bromide.

Library Generation and Illumina Sequencing

Purified ChIP DNA was used to prepare Illumina multiplexed sequencing libraries. Libraries for Illumina sequencing were prepared following the Illumina-compatible NEXTflex ChIP-seq Kit (Bioo Scientific), as described in Supplemental Experimental Procedures. The libraries were sequenced on an Illumina HiSeq 2000 to generate 50 base reads.

Data Analysis

All ChIP-seq data sets were aligned using Bowtie (version 0.12.8) (Langmead et al., 2009) to the human reference genome (GRCh37/hg19). The alignment files were analyzed with MACS2 v. 2.0.10 using a 0.001 q value cutoff (Zhang et al., 2008) to identify the p53 binding peaks. The ratio of the peak pileup between 8 and 0 hr samples was used to estimate activated p53 bindings at 8 hr after DNA damage. The ratio of the peak pileup between 16 and 8 hr was used to determine reduced p53 binding at 16 hr after DNA damage. The peaks identified by ChIP-seq were analyzed with the R Bioconductor package, ChIPpeakAnno (Zhu et al., 2010), to retrieve the nearest Ensembl gene (10 kb around TSS).

The Multiple EM for Motif Elicitation (MEME) algorithm was used to identify enriched sequence motifs in p53 binding data with sequences ± 300 bp around the summit of the peaks at 0, 8, and 16 hr after DNA damage (Bailey and Elkan, 1994). Since p53 is known to bind a 20-mer sequence, we ran MEME with parameters to allow for discovery of motifs between 18 and 24 bp in length. We used the k-means clustering function of the Cistrome "Heatmap" tool (Liu et al., 2011) to display p53 ChIP-seq levels on heatmaps. In this analysis, the signal profiles from 0, 8, and 16 hr were entered into Cistrome along with a BED file containing the genomic regions centered at the summits of p53 peaks at 8 hr after DNA damage to generate heatmaps. In the heatmap representation, each row represents the ±2.5 kb centered on the summit of p53 enriched peak and ranked according to the enrichment of p53 occupancy at 8 hr after DNA damage.

RT-PCR and RT-qPCR

Total RNA was extracted using either TRIzol reagent (Sigma) or AllPrep DNA/RNA mini kit (QIAGEN) according to manufacturer's protocol. RT-PCR was performed using SuperScript One-Step RT-PCR kit (Invitrogen). RT-qPCR was performed using iQ SYBR Green Supermix and iScript cDNA synthesis kit on CFX96 Real Time System (Bio-Rad). Primer sets for amplification of p21 mRNA are 5′-CGACTGTGATGCGCTAATGG and 5′-GGCGTTTGGAGT GGTAGAAATC; for p21 hnRNA, they are 5′- GACACAGCAAAGCCCGGCCA and 5′-CAACTCATCCCGGCCTCGCC; and for PIG1 hnRNA, they are 5′-TGCTCATCATCGCGTCAG and 5′-GCTTTGCCCAACCCTCT.

Cell Apoptosis Analysis

U2OS cells were subjected to UV radiation (10 J/m^2) and collected 24 hr after UV treatment. They were then fixed, stained with propidium iodide, and analyzed by FACScan flow cytometry (Becton Dickinson) for apoptotic cells (SubG1) according to DNA content.

ACCESSION NUMBERS

All ChIP-seq data are deposited in EBI under accession number E-MTAB-1988.

SUPPLEMENTAL INFORMATION

Supplemental Information includes six figures, two tables, and Supplemental Experimental Procedures and can be found with this article online at http://dx.doi.org/10.1016/j.molcel.2013.10.031.

ACKNOWLEDGMENTS

We are very grateful to Dr. R.G. Roeder and all members of our laboratory, particularly Dr. A.G. Li, for valuable suggestions and helpful discussion. We thank Dr. J. Shyy for providing Ad-DN-AMPK adenovirus, Dr. E. Wang for providing TAF4 antibody, Dr. E. Martinez for providing TAF5 antibody, and D. Niks for assistance in K_m analysis. This work was supported by NIH grant R01CA075180 to X.L., American Heart Association postdoctoral fellowship POST3530033 to Y.W., NIH postdoctoral fellowship F32CA144214 to J.C.L., and NIH predoctoral fellowship F31CA177219 to S.B.

Received: February 11, 2013
Revised: October 1, 2013
Accepted: October 25, 2013
Published: November 27, 2013

REFERENCES

Amé, J.C., Spenlehauer, C., and de Murcia, G. (2004). The PARP superfamily. Bioessays *26*, 882–893.

Bailey, T.L., and Elkan, C. (1994). Fitting a mixture model by expectation maximization to discover motifs in biopolymers. Proc. Int. Conf. Intell. Syst. Mol. Biol. *2*, 28–36.

Beck, M., Schmidt, A., Malmstroem, J., Claassen, M., Ori, A., Szymborska, A., Herzog, F., Rinner, O., Ellenberg, J., and Aebersold, R. (2011). The quantitative proteome of a human cell line. Mol. Syst. Biol. *7*, 549.

Bode, A.M., and Dong, Z. (2004). Post-translational modification of p53 in tumorigenesis. Nat. Rev. Cancer *4*, 793–805.

Boulton, S., Kyle, S., and Durkacz, B.W. (1999). Interactive effects of inhibitors of poly(ADP-ribose) polymerase and DNA-dependent protein kinase on cellular responses to DNA damage. Carcinogenesis *20*, 199–203.

Burley, S.K., and Roeder, R.G. (1996). Biochemistry and structural biology of transcription factor IID (TFIID). Annu. Rev. Biochem. *65*, 769–799.

Cai, X., and Liu, X. (2008). Inhibition of Thr-55 phosphorylation restores p53 nuclear localization and sensitizes cancer cells to DNA damage. Proc. Natl. Acad. Sci. USA *105*, 16958–16963.

Dennis, P.B., Jaeschke, A., Saitoh, M., Fowler, B., Kozma, S.C., and Thomas, G. (2001). Mammalian TOR: a homeostatic ATP sensor. Science *294*, 1102–1105.

Dikstein, R., Ruppert, S., and Tjian, R. (1996). TAFII250 is a bipartite protein kinase that phosphorylates the base transcription factor RAP74. Cell *84*, 781–790.

Dong, F., Soubeyrand, S., and Haché, R.J.G. (2010). Activation of PARP-1 in response to bleomycin depends on the Ku antigen and protein phosphatase 5. Oncogene *29*, 2093–2103.

Ethier, C., Tardif, M., Arul, L., and Poirier, G.G. (2012). PARP-1 modulation of mTOR signaling in response to a DNA alkylating agent. PLoS ONE *7*, e47978.

Gribble, F.M., Loussouarn, G., Tucker, S.J., Zhao, C., Nichols, C.G., and Ashcroft, F.M. (2000). A novel method for measurement of submembrane ATP concentration. J. Biol. Chem. *275*, 30046–30049.

Guertin, D.A., and Sabatini, D.M. (2009). The pharmacology of mTOR inhibition. Sci. Signal. *2*, pe24.

Ha, H.C., and Snyder, S.H. (1999). Poly(ADP-ribose) polymerase is a mediator of necrotic cell death by ATP depletion. Proc. Natl. Acad. Sci. USA *96*, 13978–13982.

Hardie, D.G. (2007). AMP-activated/SNF1 protein kinases: conserved guardians of cellular energy. Nat. Rev. Mol. Cell Biol. *8*, 774–785.

Horton, J.K., Stefanick, D.F., Naron, J.M., Kedar, P.S., and Wilson, S.H. (2005). Poly(ADP-ribose) polymerase activity prevents signaling pathways for cell cycle arrest after DNA methylating agent exposure. J. Biol. Chem. *280*, 15773–15785.

Inoki, K., Zhu, T., and Guan, K.L. (2003). TSC2 mediates cellular energy response to control cell growth and survival. Cell *115*, 577–590.

Jacobson, R.H., Ladurner, A.G., King, D.S., and Tjian, R. (2000). Structure and function of a human TAFII250 double bromodomain module. Science *288*, 1422–1425.

Jones, R.G., Plas, D.R., Kubek, S., Buzzai, M., Mu, J., Xu, Y., Birnbaum, M.J., and Thompson, C.B. (2005). AMP-activated protein kinase induces a p53-dependent metabolic checkpoint. Mol. Cell *18*, 283–293.

Kim, T.H., Barrera, L.O., Zheng, M., Qu, C., Singer, M.A., Richmond, T.A., Wu, Y., Green, R.D., and Ren, B. (2005). A high-resolution map of active promoters in the human genome. Nature *436*, 876–880.

Knight, Z.A., and Shokat, K.M. (2005). Features of selective kinase inhibitors. Chem. Biol. *12*, 621–637.

Kruse, J.P., and Gu, W. (2009). Modes of p53 regulation. Cell *137*, 609–622.

Langmead, B., Trapnell, C., Pop, M., and Salzberg, S.L. (2009). Ultrafast and memory-efficient alignment of short DNA sequences to the human genome. Genome Biol. *10*, R25.

Li, H.-H., Li, A.G., Sheppard, H.M., and Liu, X. (2004). Phosphorylation on Thr-55 by TAF1 mediates degradation of p53: a role for TAF1 in cell G1 progression. Mol. Cell *13*, 867–878.

Li, A.G., Piluso, L.G., Cai, X., Gadd, B.J., Ladurner, A.G., and Liu, X. (2007a). An acetylation switch in p53 mediates holo-TFIID recruitment. Mol. Cell *28*, 408–421.

Li, H.-H., Cai, X., Shouse, G.P., Piluso, L.G., and Liu, X. (2007b). A specific PP2A regulatory subunit, B56γ, mediates DNA damage-induced dephosphorylation of p53 at Thr55. EMBO J. *26*, 402–411.

Liu, X., and Berk, A.J. (1995). Reversal of in vitro p53-squelching by both TFIIB and TFIID. Mol. Cell Biol. *15*, 6471–6478.

Liu, T., Ortiz, J.A., Taing, L., Meyer, C.A., Lee, B., Zhang, Y., Shin, H., Wong, S.S., Ma, J., Lei, Y., et al. (2011). Cistrome: an integrative platform for transcriptional regulation studies. Genome Biol. *12*, R83.

Narkar, V.A., Downes, M., Yu, R.T., Embler, E., Wang, Y.X., Banayo, E., Mihaylova, M.M., Nelson, M.C., Zou, Y., Juguilon, H., et al. (2008). AMPK and PPARdelta agonists are exercise mimetics. Cell *134*, 405–415.

O'Brien, T., and Tjian, R. (1998). Functional analysis of the human TAFII250 N-terminal kinase domain. Mol. Cell *1*, 905–911.

Schreiber, V., Dantzer, F., Ame, J.C., and de Murcia, G. (2006). Poly(ADP-ribose): novel functions for an old molecule. Nat. Rev. Mol. Cell Biol. *7*, 517–528.

Sekiguchi, T., Nohiro, Y., Nakamura, Y., Hisamoto, N., and Nishimoto, T. (1991). The human CCG1 gene, essential for progression of the G1 phase, encodes a 210-kilodalton nuclear DNA-binding protein. Mol. Cell. Biol. *11*, 3317–3325.

Thomas, M.C., and Chiang, C.M. (2006). The general transcription machinery and general cofactors. Crit. Rev. Biochem. Mol. Biol. *41*, 105–178.

Tora, L. (2002). A unified nomenclature for TATA box binding protein (TBP)-associated factors (TAFs) involved in RNA polymerase II transcription. Genes Dev. *16*, 673–675.

Vander Heiden, M.G., Cantley, L.C., and Thompson, C.B. (2009). Understanding the Warburg effect: the metabolic requirements of cell proliferation. Science *324*, 1029–1033.

Vousden, K.H., and Prives, C. (2009). Blinded by the light: the growing complexity of p53. Cell *137*, 413–431.

Wang, E.H., and Tjian, R. (1994). Promoter-selective transcriptional defect in cell cycle mutant ts13 rescued by hTAFII250. Science *263*, 811–814.

Warburg, O. (1956). On the origin of cancer cells. Science *123*, 309–314.

Zhang, Y., Liu, T., Meyer, C.A., Eeckhoute, J., Johnson, D.S., Bernstein, B.E., Nusbaum, C., Myers, R.M., Brown, M., Li, W., and Liu, X.S. (2008). Model-based analysis of ChIP-Seq (MACS). Genome Biol. *9*, R137.

Zhou, G., Myers, R., Li, Y., Chen, Y., Shen, X., Fenyk-Melody, J., Wu, M., Ventre, J., Doebber, T., Fujii, N., et al. (2001). Role of AMP-activated protein kinase in mechanism of metformin action. J. Clin. Invest. *108*, 1167–1174.

Zhu, L.J., Gazin, C., Lawson, N.D., Pagès, H., Lin, S.M., Lapointe, D.S., and Green, M.R. (2010). ChIPpeakAnno: a bioconductor package to annotate ChIP-seq and ChIP-chip data. BMC Bioinformatics *11*, 237.